

VLTI/MIDI observation of the silicate carbon star IRAS08002-3803: Silicate dust reservoir spatially resolved for the first time

K. Ohnaka^a, T. Driebe^a, K.-H. Hofmann^a, Th. Preibisch^a, D. Schertl^a, G. Weigelt^a,
M. Wittkowski^b

^a Max-Planck-Institut für Radioastronomie, D-53121 Bonn, Germany

Contact: kohnaka@mpifr-bonn.mpg.de

^b European Southern Observatory, D-85748 Garching, Germany

1. Introduction

The dust species formed in the circumstellar envelope around asymptotic giant branch (AGB) stars reflect the chemical composition of the photosphere. Dust grains such as silicate and corundum (Al_2O_3) are observed around oxygen-rich stars (M giants), while amorphous carbon and/or silicon carbide (SiC) are observed around carbon stars. However, carbon stars showing (amorphous) silicate emission were discovered in the IRAS Low Resolution Spectra (LRS) by Little-Marein (1986, ApJ, 307, L15) and Willems & de Jong (1986, ApJ, 309, L39). At the moment, the most widely accepted hypothesis suggests that silicate carbon stars have a low-luminosity companion, and that oxygen-rich material was shed by mass loss when the primary star was an M giant and this oxygen-rich material is stored in a circumbinary disk until the primary star becomes a carbon star (Morris 1987, PASP, 99, 1115; Lloyd-Evans 1990, MNRAS, 243, 336) or in a circumstellar disk around the companion (Yamamura et al. 2000, A&A, 363, 629). However, this scenario is neither rejected nor confirmed. Here we present the results of the first *N*-band spectro-interferometric observations of the silicate carbon star Hen 38 (IRAS08002-3803) with VLTI/MIDI.

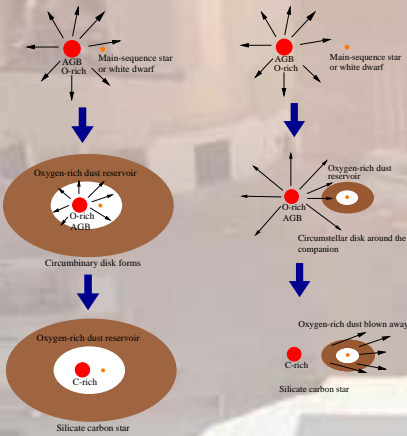


Fig. 1: Left: Scenario A for the formation of a silicate carbon star (Morris 1987, Lloyd-Evans 1990). Right: Scenario B for the formation of a silicate carbon star. Yamamura et al. (2000).

2. MIDI observations of Hen 38

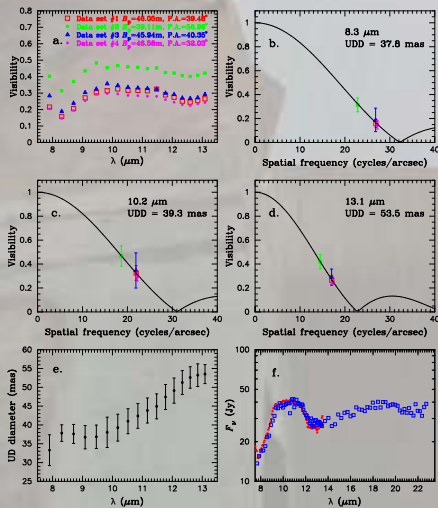


Fig. 2: *N*-band visibilities and spectra observed for Hen 38. MIDI observations: 2004 February, prism mode ($\lambda/\Delta\lambda \approx 30$), SDT program. Data reduction: MIA+EWS package. The average values derived with both packages are plotted. a: MIDI visibilities plotted as a function of wavelength. The error bars are omitted for the sake of visual clarity. b-d: Visibilities plotted as a function of spatial frequency. Uniform disk fits are also shown. e: Uniform-disk diameter derived from the MIDI observations f: Observed spectra of Hen 38. Filled circles: MIDI spectrum. Open squares: IRAS LRS.

An unexpected wavelength dependence: the angular size remains constant (~36 mas) from 8 to 10 μm , in spite of the very prominent rise of silicate emission, and a rather steep increase longward of 10 μm to reach ~55 mas at 13 μm .

3. Modeling with silicate dust alone

We first examine axisymmetric silicate disk models whose geometry is depicted in the inset of Fig. 3a. SEDs and *N*-band images and visibilities are calculated with a Monte Carlo radiative transfer code (Ohnaka et al. 2006, A&A, 1015, 1029). Figure 3a shows an example of models which can reproduce the observed SED rather well. However, Fig. 3c reveals that the model visibilities fail to reproduce the visibilities observed with MIDI. The silicate disk model predicts the angular size of the object to increase steeply from 8 to 10 μm , while the observed angular size remains roughly constant longward of 10 μm .

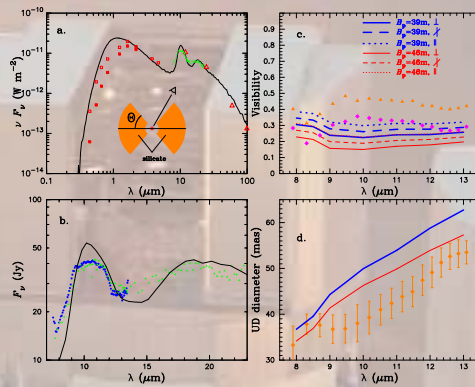


Fig. 3: Results for an axisymmetric disk model consisting of silicate dust alone. Model parameters: disk half-opening angle = 50° , inner radius = $15 R_*$ (30 AU), optical depth at $0.55 \mu\text{m}$ = 15 in the equatorial direction. Dust density $\propto r^{-1.4}$. Viewing angle = 30° from pole-on. a: The observed SED by the open squares (Le Bertre et al. 1990, de-reddened with $A_V = 1.5$), open triangles (IRAS), and filled triangles (IRAS LRS). The original data of Le Bertre et al. (1990), not corrected for the interstellar extinction, are also plotted with the filled squares. The model SED is represented with the solid line. b: Filled triangles (IRAS LRS), filled circles (MIDI spectrum), solid line: model spectrum. c: The visibilities measured with the 39 m (filled triangles) and 46 m baselines (filled diamonds). The corresponding model visibilities are plotted with the thick and thin solid lines. The solid, dashed, and dotted lines represent the model visibilities predicted for different position angles (solid line: perpendicular to the symmetry axis of the model intensity distribution, dotted line: parallel to the symmetry axis, dashed line: 45° with respect to the symmetry axis). See also Fig. 5 for the illustration of the orientation of the baseline vectors. d: Filled diamonds: observed uniform-disk diameters. Thick and thin solid lines: model uniform-disk diameters for the 39 m and 46 m baselines, respectively, with the baseline vector perpendicular to the symmetry axis of the disk.

How the unexpected wavelength dependence of the observed visibility can be explained?

⇒ Two grain species: silicate + ?

⇒ Second grain species candidates: amorphous carbon, large silicate grains, and metallic iron

⇒ Radiative transfer calculations, comparison with the observed SED and *N*-band visibilities

⇒ Models with these two grain species can fairly – though not entirely satisfactorily – reproduce the observed SED and MIDI observations. See Ohnaka et al. (2006, A&A, 1015, 1029) for details.

4. Model with silicate and metallic iron

We present one of the three two-grain-species models we considered: the silicate + metallic iron model. In this model, silicate and metallic iron grains coexist throughout the disk. Figure 4 shows the result obtained by such a model. The optical depths of silicate and metallic iron dust used in this best-fit model are 20 and 3.0, respectively (1.5 and 0.34 at 10 μm , respectively). The observed SED as well as the *N*-band visibilities are fairly reproduced. The intensity distributions of the silicate and metallic iron components show different angular sizes and wavelength dependences, and the flux contributions of these two components also vary in the *N*-band, particularly due to the 10 μm silicate feature. The combination of these factors results in a wavelength dependence of the *N*-band visibility totally different from that predicted by the models with silicate dust alone.

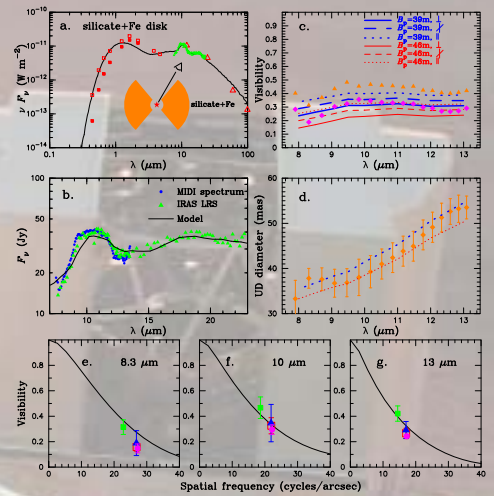


Fig. 4: The best-fit model containing silicate and metallic iron dust. Model parameters: Disk half-opening angle = 50° , $\tau(V)(\text{silicate}) = 20$, $\tau(V)(\text{Fe}) = 3.0$, $r_{\text{in}}(\text{silicate}) = 20 R_*$ (40 AU), dust density (silicate, metallic iron) $\propto r^{-1.6}$. Viewing angle = 30° from pole-on. See also the legend to Fig. 3 for the references of the symbols.

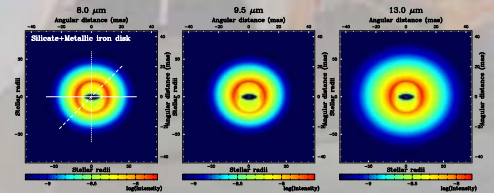


Fig. 5: The mid-infrared images predicted by the silicate+Fe dust model for 8 μm , 9.5 μm , and 13 μm . In each image, the color scale is normalized with the maximum intensity (excluding the central star) and the minimum intensity set to $3 \times 10^{-2} \times$ maximum intensity (the color scale on the central star is saturated). The solid, dashed, and dotted lines in the left panel illustrate the orientation of the baseline vectors used in the visibility calculations.

5. Concluding remarks

- Our MIDI observations resolved the dusty environment of a silicate carbon star, Hen 38, for the first time.
- Neither spherical shell models nor axisymmetric disk models consisting of silicate dust alone can explain the observed SED and *N*-band visibilities of Hen 38.
- Disk models with two grain species, silicate and a second grain species such as amorphous carbon, large silicate grains, and metallic iron grains, can fairly reproduce the observations. However, the agreement with the observed *N*-band visibilities is not yet entirely satisfactory, which suggests more complicated disk geometries and/or spatial variation of dust chemistry (i.e., distinct regions of the disk are populated with different grain species due to dust formation and growth processes).
- Our MIDI observations and radiative transfer modeling lends support to the presence of a circumbinary disk around Hen 38.